Lawrence Berkeley Laboratory
UNIVERSITY OF CALIFORNIA

Presented at the Society of Nuclear Medicine 26th Annual Meeting, Atlanta, GA, June 26-29, 1979

EMISSION AND TRANSMISSION NOISE PROPAGATION IN POSITRON EMISSION COMPUTED TOMOGRAPHY

Grant T. Gullberg and Ronald H. Huesman

June 1979

Prepared for the U.S. Department of Energy under Contract W-7405-ENG-48

Presented at the Society of Nuclear Medicine 26th Annual Meeting, Atlanta, Georgia, June 1979.

LBL-9783

EMISSION AND TRANSMISSION NOISE PROPAGATION IN POSITRON EMISSION COMPUTED TOMOGRAPHY

Grant T. Gullberg and Ronald H. Huesman

DONNER LABORATORY

June 1979

Prepared for the U. S. Department of Energy under Contract W-7405-ENG-48

LBL-9783

EMISSION AND TRANSMISSION NOISE PROPAGATION IN POSITRON EMISSION COMPUTED TOMOGRAPHY

Grant T. Gullberg and Ronald H. Huesman

Donner Laboratory
Lawrence Berkeley Laboratory
University of California
Berkeley, California 94720

June 1979

ABSTRACT

Errors in positron emission computed tomograms are the result of noise propagated from three sources: 1) the statistical fluctuation in the positron coincidence events; 2) the statistical fluctuation in the incident transmission beam; and 3) the statistical fluctuation in the transmitted beam. The data for the transmission study in 2) and 3) are used to compensate for internal absorption of the distributed positron source. For the reconstruction of a circular phantom using the convolution algorithm, the percent root-mean-square uncertainty (%RMS) is related to the total measured positron events C and the incident photon flux per cm I_0. Our derivation of the %RMS uncertainty based on the propagation of errors yields a simple expression: $\%RMS = \sqrt{K_1/C + K_2/I_0}$ where K_1 and K_2 are constants dependent on the size of the object and the type of convolver.

The constants $K_1 = 4.52 \times 10^8$ and $K_2 = 1.48 \times 10^8$ were determined for a 20 cm diameter disc based on computer simulation with various emission and transmission statistics. The projection data were analytically calculated with an attenuation coefficient $\mu = 0.0958\ cm^{-1}$ for 140 angles between 0 and π. Poisson noise was added to the positron coincidence events, the incident transmission events I_0, and the transmitted events. These results indicate that for a total number of incident transmission photons per cm of 2.0×10^5, the contrast resolution for a fixed spatial resolution is limited to 27% even with an infinite number of emission events. For a total of 10^6 emission events the contrast resolution is 34%.

INTRODUCTION

The propagation of errors for positron emission computed tomography can be formulated for the convolution algorithm. The mean and variance of the reconstructed density ρ at the point (x,y) in the cross-sectional image is given by

$$E\{\rho(x,y)\} = \mathcal{B}\{c(\xi) * E[p(\xi,\theta)]\} \tag{1}$$

$$\mathrm{Var}\{\rho(x,y)\} = \mathcal{B}\{c^2(\xi) * \mathrm{Var}[p(\xi,\theta)]\} \tag{2}$$

where $c(\xi)$ is the convolution function, $p(\xi,\theta)$ is the projected data input to the convolution algorithm, and $\mathcal{B}$ denotes the back-projection operation. Using these two equations we have an expression for the percent root-mean-square uncertainty (%RMS) as

$$\%\ \mathrm{RMS} = \frac{100\ \mathcal{B}^{\frac{1}{2}}\{c^2(\xi) * \mathrm{Var}[p(\xi,\theta)]\}}{\mathcal{B}\{c(\xi) * E[p(\xi,\theta)]\}} \ . \tag{3}$$

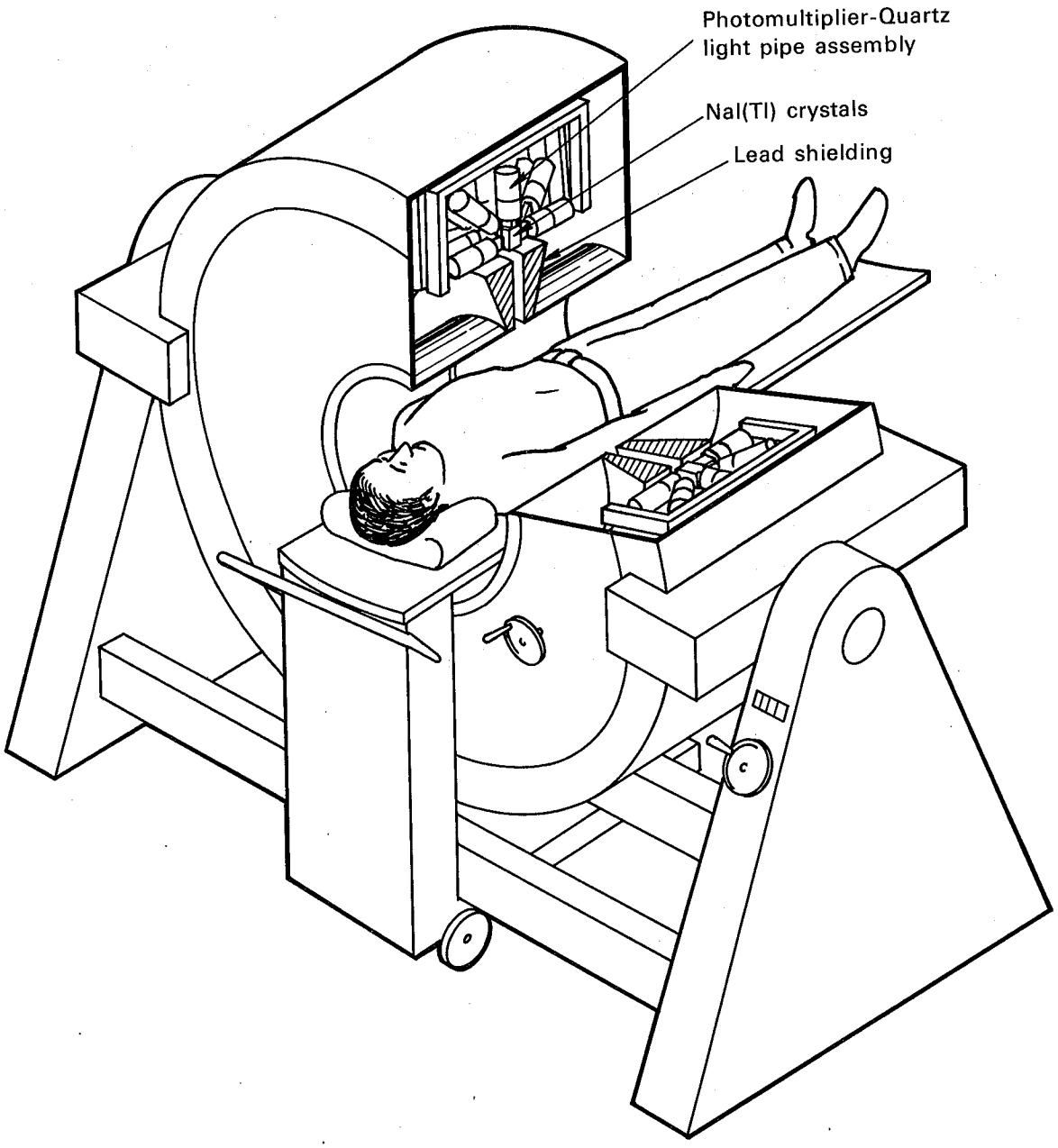

Figure 1. Schematic of Donner 280-Crystal Positron Tomograph. (Derenzo, Budinger, Cahoon, Huesman, and Jackson, 1977).

SOURCES OF ERRORS

Statistical fluctuation in the sampled projections come from three sources:

(1) fluctuations in the measured coincidence events $p_{\gamma\gamma}(\xi,\theta)$;

(2) fluctuations in the incident transmission beam I_o;

(3) fluctuations in the measured transmitted beam $I(\xi,\theta)$.

The projections, $p(\xi,\theta)$, which are input to the convolution reconstruction algorithm are related to the measurements $p_{\gamma\gamma}(\xi,\theta)$, I_o, and $I(\xi,\theta)$ by the equation

$$p(\xi,\theta) = p_{\gamma\gamma}(\xi,\theta) \frac{I_o}{I(\xi,\theta)} \tag{4}$$

where I_o and I are incident and transmitted photon flux, respectively, and their quotient is used to correct the number of measured emission events for attenuation losses. If we assume that all measured variants satisfy Poisson statistics, the mean for $p(\xi,\theta)$ is given by

$$E\{p(\xi,\theta)\} = p_{\gamma\gamma} \frac{I_o}{I(\xi,\theta)} \tag{5}$$

where $E\{1/I(\xi,\theta)\} \simeq 1/E\{I(\xi,\theta)\}$ and the variance for $p(\xi,\theta)$ is given by

$$\begin{aligned} \mathrm{Var}\{p(\xi,\theta)\} &= \left(\frac{\partial p}{\partial I_o}\right)^2 \mathrm{Var}(I_o) + \left(\frac{\partial p}{\partial I}\right)^2 \mathrm{Var}(I) + \left(\frac{\partial p}{\partial p_{\gamma\gamma}}\right)^2 \mathrm{Var}(p_{\gamma\gamma}) \\ &= \frac{I_o\, p_{\gamma\gamma}(\xi,\theta)}{I(\xi,\theta)^3} \left(p_{\gamma\gamma}(\xi,\theta)\, I(\xi,\theta) + p_{\gamma\gamma}(\xi,\theta) I_o + I_o\, I(\xi,\theta)\right) \end{aligned} \tag{6}$$

The reconstructed % RMS uncertainty for any phantom can be evaluated by substituting Eqs. (5) and (6) into Eq. (3).

ERRORS FOR A DISC OF UNIFORM CONCENTRATION AND UNIFORM ATTENUATOR

As an example, consider a circular disc with radius R. The projections for the disc with a distributed positron source can be calculated analytically as

$$p_{\gamma\gamma}(\xi,\theta) = \begin{cases} 2\rho\sqrt{R^2-\xi^2}\,\exp(-2\mu\sqrt{R^2-\xi^2}) = \rho\, L(\xi)\, e^{-\mu L(\xi)}, & |\xi| \le R \\ 0 & \text{otherwise} \end{cases} \tag{7}$$

where ρ is the concentration of positron emitter, μ is the attenuation coefficient, and $L(\xi) = 2\sqrt{R^2-\xi^2}$. The projections $P_{\gamma\gamma}(\xi,\theta)$ are plotted for different size discs in Fig. 2. For the same disc with uniform attenuation, the transmission data has a measured transmitted beam intensity given by

$$I(\xi,\theta) = \begin{cases} I_0\,\exp(-2\mu\sqrt{R^2-\xi^2}) = I_0\, e^{-\mu L(\xi)} & |\xi| \le R \\ 0 & \text{otherwise} \end{cases} \tag{8}$$

Substituting Eqs. (7) and (8) into Eqs. (5) and (6) gives the mean and variance for the projections $p(\xi,\theta)$ which are used by the convolution algorithm:

$$E\{p(\xi,\theta)\} = \rho\, L(\xi), \tag{9}$$

$$\mathrm{Var}\{p(\xi,\theta)\} = \frac{\rho\, L(\xi)\, e^{\mu L(\xi)}}{I_0}\,[I_0+\rho\, L(\xi)(1+e^{-\mu L(\xi)})]. \tag{10}$$

Substituting Eqs. (9) and (10) into Eq. (3) gives the % RMS uncertainty as a function of ρ and I_0:

$$(\%\ \mathrm{RMS})^2 = \frac{10^4}{\rho}\,\frac{\mathcal{B}\{c^2(\xi)*[L(\xi)e^{\mu L(\xi)}]\}}{\mathcal{B}^2\{c(\xi)*L(\xi)\}} + \frac{10^4}{I_0}\,\frac{\mathcal{B}\{c^2(\xi)*[L^2(\xi)(1+e^{\mu L(\xi)})]\}}{\mathcal{B}^2\{c(\xi)*L(\xi)\}}. \tag{11}$$

The total number of emission events C is related to the concentration ρ by $C = \rho\int L(\xi)\, e^{-\mu L(\xi)} d\xi$. Parameterizing Eq. (11) as a function of C and I_0 gives

$$(\%\ \mathrm{RMS})^2 = \frac{K_1}{C} + \frac{K_2}{I_0} \tag{12}$$

where K_1 and K_2 are the corresponding factors of $1/C$ and $1/I_0$ respectively, given in Eq. (11). Therefore the % RMS uncertainty for a circular disc is a simple function of the total number of emission events C and the incident photon flux I_0.

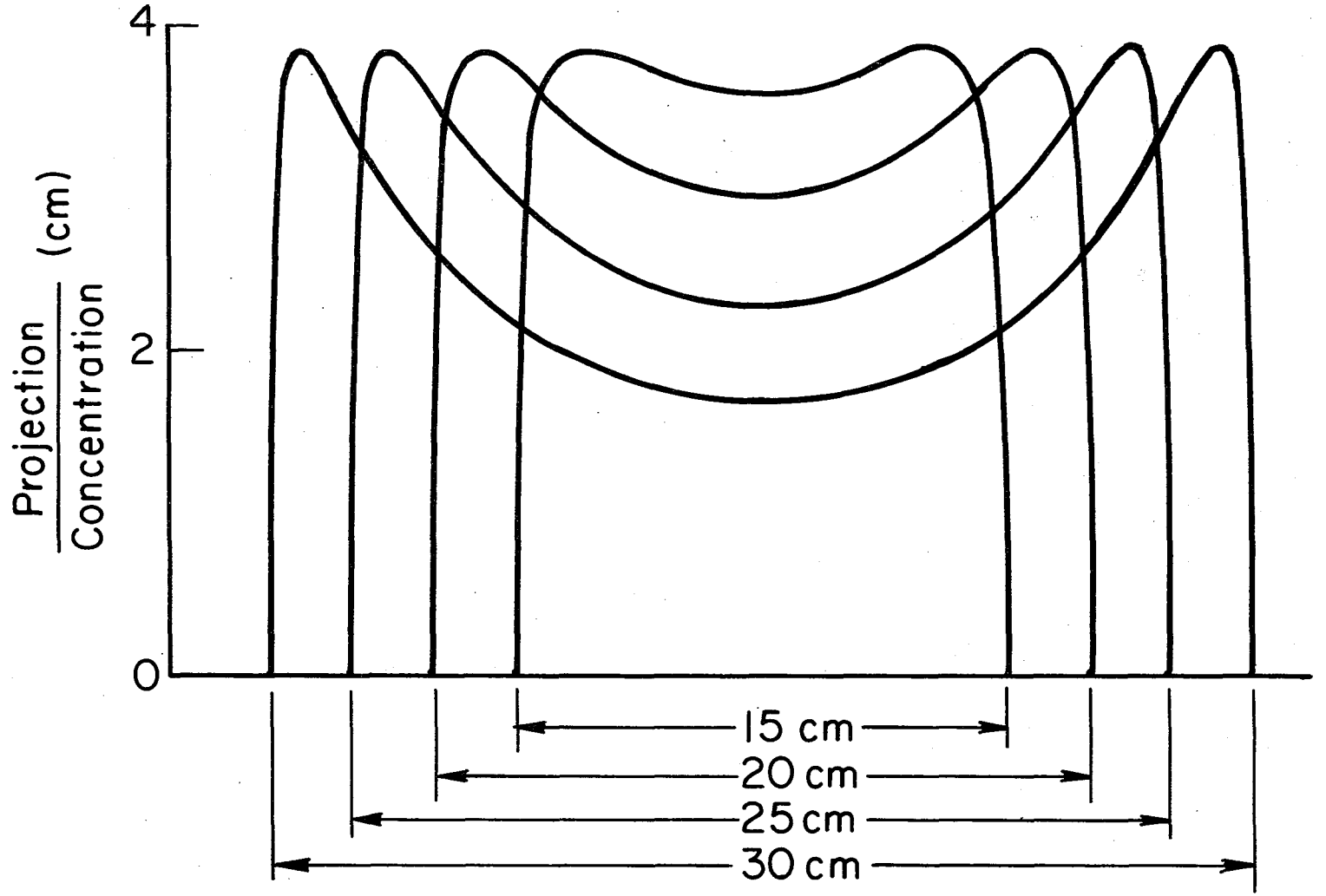

XBL796-3509

Figure 2. Projections of a uniformly distributed positron source in 15, 20, 25, and 30 cm discs (μ = .0958 cm^{-1}).

RESULTS

To evaluate the constants K_1 and K_2, simulations were done on 15, 20, 25, and 30 cm discs. The projection data were analytically calculated every .33 cm using an attenuation coefficient $\mu = 0.0958\ cm^{-1}$ for 140 angles between 0 and π. Poisson noise was assumed present in the measured projections $p_{\gamma\gamma}(\xi,\theta)$, the incident transmission flux I_o, and the measured transmission flux $I(\xi,\theta)$. The errors were reconstructed (see Huesman, Gullberg, Greenberg, Budinger, 1977) using the Shepp and Logan convolver (Shepp and Logan, 1974) and are tablulated in Table 1. Using the 30 data points for each disc size, the parameters K_1 and K_2 were evaluated using a least-squares fit.

The visual effects of noise are illustrated in Fig. 3 for a 20-cm disc with $\mu = 0.0958\ cm^{-1}$. The errors for these reconstructions are those given for the 20-cm disc in Table 1. The corresponding constants K_1 and K_2 for the 20-cm disc with attenuation coefficient $\mu = .0958\ cm^{-1}$ are $K_1 = 4.52 \times 10^8$ and $K_2 = 1.48 \times 10^8$, which allows us to express the percent RMS uncertainty in terms of the total events C and the incident number of transmission photons per cm I_o as given by the equation

$$\%RMS = \left\{ \frac{4.52 \times 10^8}{C} + \frac{1.48 \times 10^8}{I_o} \right\}^{\frac{1}{2}}$$

This equation is plotted in Fig. 4 for %RMS uncertainty of 5, 10, 20, 40, and 60%.

Percent Root-Mean-Square Uncertainty

Total Number of Emission Events (C)	Total Number of Incident Transmission Photons Per Cm (I_o)					
	2.0×10^5	4.0×10^5	8.0×10^5	1.6×10^6	3.2×10^6	∞
15-cm disc						
1.0×10^5	45.62	43.99	43.15	42.73	42.51	42.13
3.0×10^5	29.80	27.25	25.87	25.16	24.79	24.33
1.0×10^6	21.70	18.02	15.87	14.68	14.04	13.32
3.0×10^6	18.75	14.34	11.52	9.80	8.83	7.69
∞	17.09	12.08	8.54	6.04	4.27	.00
20-cm disc						
1.0×10^5	72.53	69.94	68.60	67.93	67.58	67.32
3.0×10^5	47.40	43.32	41.13	39.99	39.41	38.87
1.0×10^6	34.52	28.67	25.24	23.34	22.32	21.29
3.0×10^6	29.84	22.82	18.32	15.59	14.03	12.29
∞	27.20	19.23	13.60	9.62	6.80	.00
25-cm disc						
1.0×10^5	104.83	100.72	98.61	97.53	96.99	96.20
3.0×10^5	69.19	62.80	59.35	57.54	56.62	55.54
1.0×10^6	51.16	42.12	36.77	33.78	32.18	30.42
3.0×10^6	44.69	33.97	27.05	22.82	20.38	17.56
∞	41.08	29.05	20.54	14.52	10.27	.00
30-cm disc						
1.0×10^5	144.46	138.03	134.70	133.00	132.15	131.39
3.0×10^5	96.83	86.95	81.57	78.74	77.28	75.86
1.0×10^6	73.18	59.49	51.30	46.66	44.17	41.55
3.0×10^6	64.85	48.89	38.50	32.07	28.31	23.99
∞	60.26	42.61	30.13	21.31	15.06	.00

Table 1. Percent root-mean-square uncertainty (RMS) for 15, 20, 25, and 30 cm diameter discs reconstructed using a convolution algorithm applied to 140 equally spaced projections between 0 and π with Poisson noise. These data were fitted to the expression $\text{RMS} = \sqrt{K_1/C + K_2/I_o}$ giving the following results for the constants K_1 and K_2

	K_1	K_2
15 cm	1.79×10^8	5.86×10^7
20 cm	4.52×10^8	1.48×10^8
25 cm	9.29×10^8	3.38×10^8
30 cm	1.72×10^9	7.26×10^8

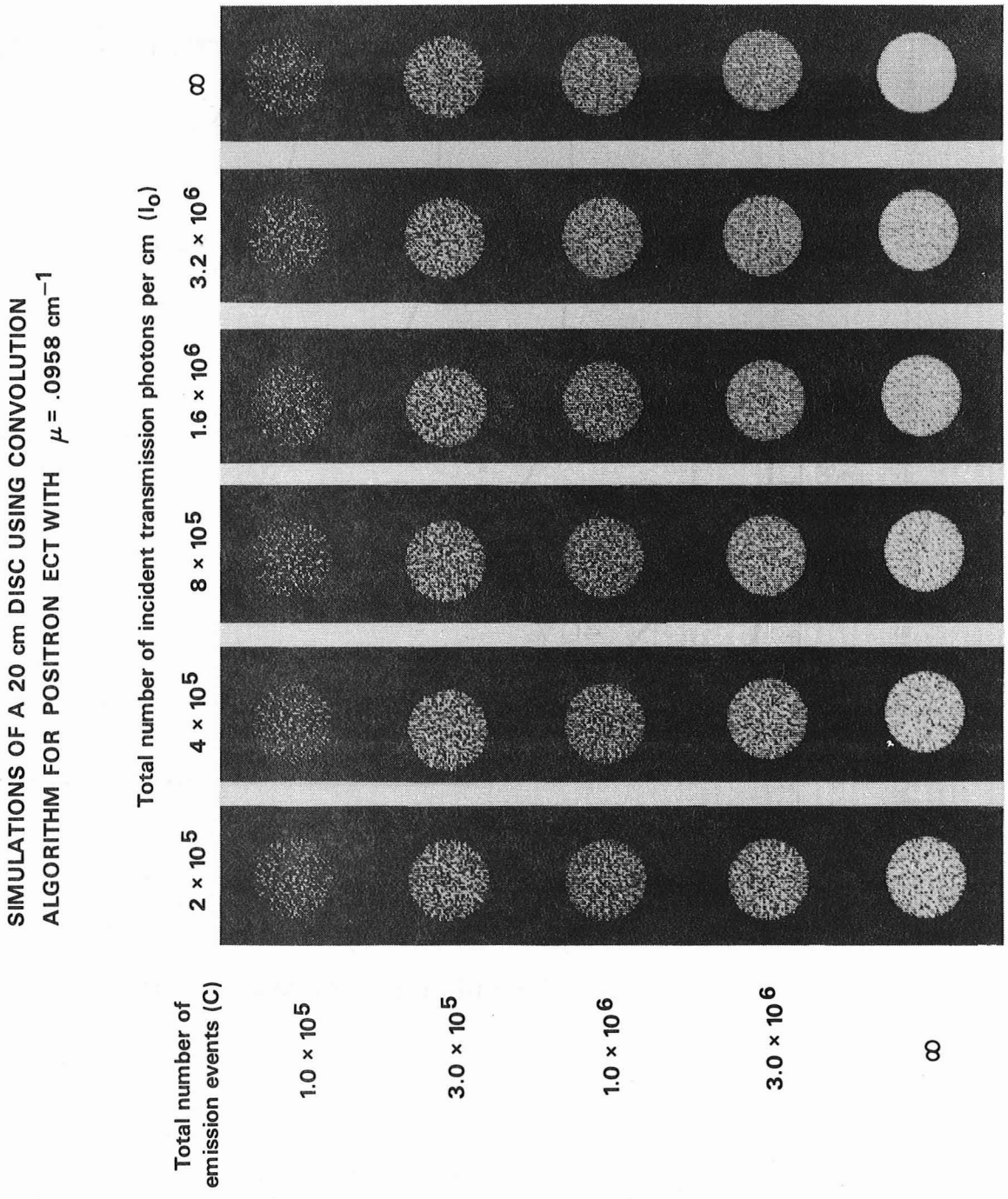

Figure 3. Reconstruction of a 20 cm disc using the Shepp and Logan convolver applied to 140 projections between 0 and π after the projections were first corrected for attenuation. The variance for these projections is given by Eq. (10). The projection bins were .33 cm and the reconstructions are displayed using a 44 x 44 grid of .5 cm pixels.

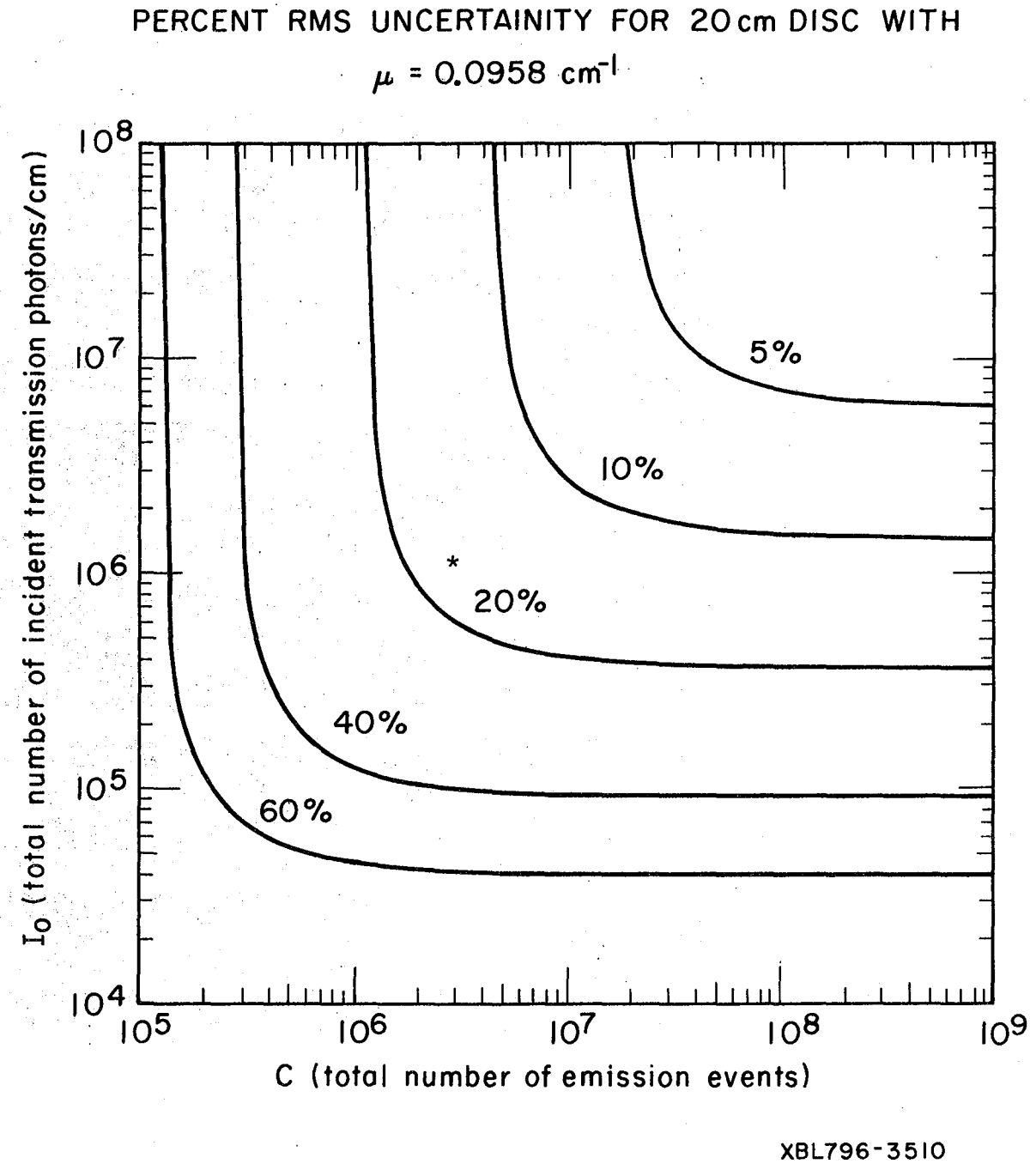

Figure 4. Percent RMS uncertainty for 20 cm disc with μ = .0958 cm^{-1}. The * indicates the % RMS uncertainty of the emission reconstruction in Figure 5.

SUMMARY

1. No matter how high the emission counts, the % RMS uncertainty of the reconstruction can be no better than $\sqrt{K_2/I_o}$. Conversely, the % RMS uncertainty is limited by $\sqrt{K_1/C}$ when transmission flux is increased.

2. As the emission counts C decrease, the rate of change of the %RMS uncertainty with respect to I_o decreases. This means that if one is not able to obtain high statistics for the emission study, then not much improvement can be expected for a transmission study with high statistics.

3. This work is applicable to reconstruction of sources distributed in a uniform attenuator such as the head or a variable attenuator such as the chest where the constants K_1 and K_2 are evaluated by putting the appropriate expressions for I_o , $I(\xi,\theta)$, and $p_{\gamma\gamma}(\xi,\theta)$ into Eq. (6). The table and figures presented here apply to the head.

4. Figure 5 shows the distribution of attenuation coefficient and positron emitter within a human head. These reconstructions we performed by the Donner Positron Tomograph. The * shown on Figure 4 indicates the % RMS uncertainty of the emission reconstruction.

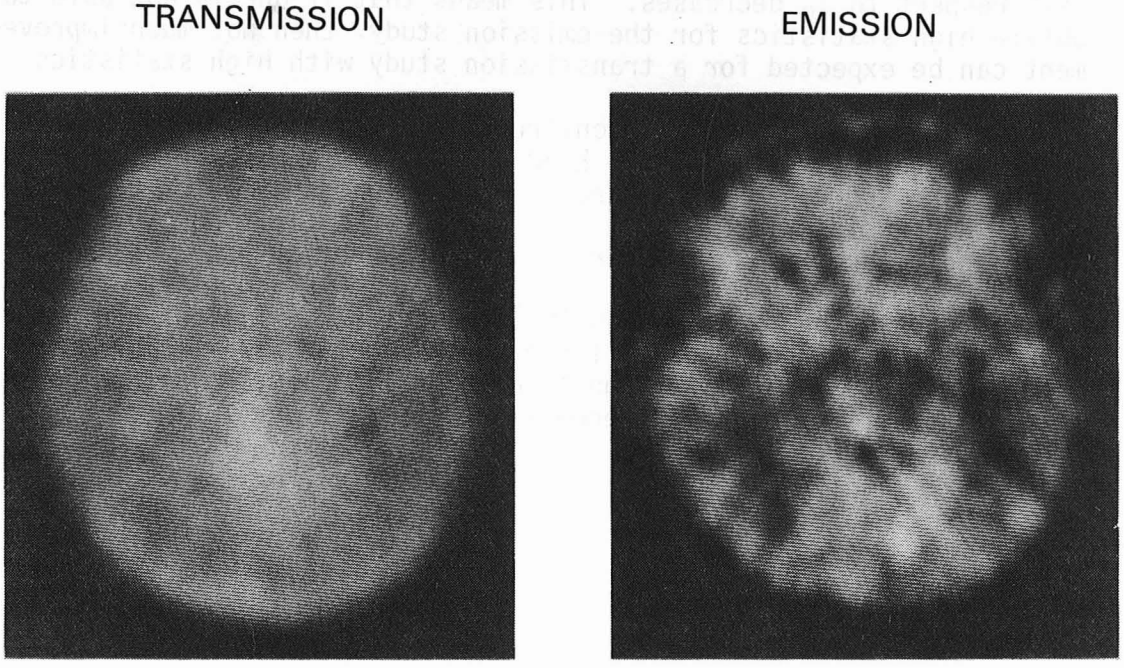

Figure 5. Reconstruction of the distribution of ^{11}C-methionine in the brain using the Donner 280-Crystal Positron Tomograph. The incident transmission flux was 1.2×10^6 photons per cm and the emission study had 2.9×10^6 events. The reconstruction algorithm used a Shepp and Logan convolver applied to projections with .5 cm projection bins after correcting for attenuation. (from Clinical Studies by Sargent and Budinger).

REFERENCES

T. F. Budinger, S. E. Derenzo, W. L. Greenberg, G. T. Gullberg, R. H. Huesman, "Quantitative Potentials of Dynamic Emission Computed Tomography," J. Nucl. Med. 19:309-315, 1978.

S. E. Derenzo, T. F. Budinger, J. L. Cahoon, R. H. Huesman, H. G. Jackson, "High Resolution Computed Tomography of Positron Emitters," IEEE Trans. Nucl. Sci. NS-24:544-558, 1977.

R. H. Huesman, G. T. Gullberg, W. L. Greenberg, T. F. Budinger, RECLBL Library Users Manual: Donner Algorithms for Reconstruction Tomography, Technical Report PUB 214, Lawrence Berkeley Laboratory, 1977.

L. A. Shepp and B. F. Logan, "The Fourier Reconstruction of a Head Section," IEEE Trans. Nucl. Sci. NS-21:21-43, 1974.

TECHNICAL INFORMATION DEPARTMENT
LAWRENCE BERKELEY LABORATORY
UNIVERSITY OF CALIFORNIA
BERKELEY, CALIFORNIA 94720